

Spectra of light reflected by aggregate structures of submicron particles

Victor P. Tishkovets^{a,b} and Elena V. Petrova^c

^a *Institute of Radio Astronomy, Kharkiv, Ukraine*

^b *V.N. Karazin Kharkiv National University, Kharkiv, Ukraine*

^c *Space Research Institute, Moscow, Russia*

emails: tishkovets@rian.kharkov.ua; epetrova@iki.rssi.ru

Abstract

We analyze the results of numerically exact computer modeling of spectral dependences of the intensity of light scattered by different aggregates of submicron spherical particles in the visible range and compare them to those of individual homogeneous spheres. The computations are performed using the Lorenz–Mie theory and the superposition T-matrix methods for aggregates, respectively. We show that, in the spectra of aggregates, along with the interference extrema peculiar of individual constituents, an additional maximum appears at longer wavelengths. The latter is considered as manifestation of collective effects in aggregate structures and can be explained by the interference of waves singly scattered by aggregate constituents that form groups along the incident radiation direction. In the spectra of randomly oriented fractal-like aggregates, this maximum becomes narrower with increasing the number of constituents and, starting from some number, its position becomes almost resistant to the further growth of aggregates and sensitive only to the refractive index and sizes of constituents. The number of constituents providing a stable collective maximum is higher for fluffier structures. In comparison with rather densely packed clusters, sparser ones exhibit the less expressed collective maximum with a slope weakly declining to the long-wavelength range. In the spectra of clusters containing particles with slightly varied sizes, the collective maximum survives, while the interference features induced by individual constituents naturally become smoother.

Keywords: light scattering, spectrum, aggregate, MSTM modeling

Highlights:

- Spectra of light reflected by fractal clusters of submicron particles are analyzed
- Interference of waves singly scattered by constituents induces new collective details
- Collective maximum is resistant to increasing the constituent number after some value
- Number of constituents providing a stable collective maximum depends of the structure
- Collective maximum is rather weakly affected by variations in the constituent sizes

1
2
3
4
5
6
7
8
9
10
11
12
13
14
15
16
17
18
19
20
21
22
23
24
25
26
27
28
29
30
31
32
33
34

1. Introduction

Characteristics of the electromagnetic radiation scattered by aggregates of submicron particles are in the focus of many studies in different application, from astrophysics to biology and from materials science to medicine [1-4]. It is often impossible to directly measure the properties of these aggregates (or clusters) of particles, and one have to conclude about their sizes, morphology, and material from the measurements of intensity and polarization of the scattered light. Results of spectral measurements also serve as a source of information on the properties of examined media. The spectral dependences are important, for example, for interpretation of observations of cometary dust or different smokes, the particles of which are aggregates of different morphology. At the same time, when interpreting the spectra, contrary to, for example, polarimetry, the structure of particles is often ignored.

However, recent studies, both theoretical and experimental, show that morphology of particles substantially influences their transmittance/absorption spectra [5–8]. In these papers, the main attention is payed to the IR spectral range and integral characteristics, such as the extinction and scattering cross-sections. The reflectance spectra of different systems of scatterers are considered in many papers (e.g., [9-11]), but they mostly deal with infinite media or layers of particles, while the scattering ensembles comparable to the wavelength in size remain beyond the reflectance spectrum analysis.

It is known that, if the sizes of particles composing aggregates are of the order of the wavelength or somewhat smaller, the aggregate morphology produces a noticeable effect on the angular dependence (the phase function) of intensity and polarization of the scattered light in the backscattering domain (see, e.g., [12–16]). This is caused by strengthening the collective effects in the scattering by ensembles of particles of these sizes. Thus, the spectrum of light scattered by a medium composed of aggregates should differ from that of homogeneous particles and depend on morphology of these aggregates, which makes the heterogeneity of scatterers to be necessarily accounted for in the interpretation of their spectra.

In this paper, we consider manifestations of collective effects in limited aggregate structures of submicron particles observed in the visible spectrum of intensity of the scattered radiation. The intensity depends on both the value of the phase function of particles at a specified scattering angle and their scattering cross-section. The spectral dependence of the latter is caused by the dependence of the scattering efficiency of particles Q_{sca} on their refractive index and the sizes relative to the wavelength, i.e., the size (wave) parameter $x = 2\pi a/\lambda$ (where λ is the wavelength, and a is the particle radius). The analysis of this dependence for homogeneous

1 particles are well-represented in the literature (see, e.g., [12]). The sizes of particles considered
2 here are smaller than or comparable to the visible wavelengths, which corresponds to the
3 segment of the Q_{sca} curve gradually growing with increasing x and exhibiting a gently sloping
4 hump. Thus, the details in the spectrum of the intensity of radiation scattered by particles of the
5 considered sizes should be caused mainly by the spectral behavior of the phase function of
6 particles. Consequently, it is the changes in the spectra of the phase function under the influence
7 of the structure of aggregates, the sizes of constituents, and the refractive index that is a subject
8 of the present analysis.

9 We focus here on the spectral behavior of the phase function mainly in the backscattering
10 direction $F(\pi)$ (the scattering angle is $\theta = \pi$), because this behavior provides insight into the
11 spectral dependence of the intensity of radiation scattered to the back hemisphere in a rather
12 wide range of angles. This is explained by the fact that the phase functions of clusters (as those
13 of many irregular particles) are rather smooth in the backscattering domain and exhibit no
14 pronounced features like rainbows and glories characteristic of scattering by individual spherical
15 and other regular particles. The near-field effects, which appear in the light scattering on
16 aggregates of particles, induce no sharp changes in the shape of the phase curve, while the
17 coherent backscattering on clusters of the considered sizes induces no sharp enhancement in the
18 intensity near opposition ($\theta = \pi$) (see, e.g., [14, 17]). (This statement will be illustrated below in
19 Fig. 5.)

20 The structure of the paper is as follows. First, we describe the parameters that are used in
21 the model calculations. Then, to find manifestations of collective effects in the spectra of
22 aggregates, the spectral dependences of the phase functions of single homogeneous spherical
23 particles and their aggregates are compared. The development of the collective feature identified
24 in the spectra of aggregates is analyzed with the use of definitely orientated structures containing
25 two and three spherical particles, and the changes in the spectra of fractal-like aggregates
26 induced by the increase in the number of constituent particles (CPs) are considered. The results
27 of the analysis are summarized at the end.

28 **2. Input parameters for the simulations**

29 The choice of values for the refractive index and sizes of CPs in the aggregates primarily
30 stems from the purposes of astrophysical applications. The main attention will be paid to the
31 spectral dependences of $F(\pi)$ for ice particles (the refractive index is $m = 1.33 + 0.0i$). To
32 illustrate the influence of changes in the refractive index and absorption, we also consider the so-
33 called dirty ice (the imaginary part of the refractive index was assumed at $m_i = 0.05$) and the
34 artificial material with the real part of the refractive index $m_r = 1.80$ (which approximately

1 corresponds to the mean value of m_r of Mg-Fe silicates and is close to that of tholins) and $m_i =$
2 0.10. We intentionally do not include the spectral dependence of the refractive index into our
3 analysis, because we mean to reveal a pure effect of the refractive index on the spectral pattern
4 of aggregates. At the same time, the model results for the considered values of m may be useful
5 for predicting at least a qualitative behavior of the spectrum for intermediate values of the
6 refractive index.

7 The values for the CP sizes were chosen in such a way that the size parameters of were
8 roughly between 1.0 and 2.0 for the visible spectral range. This interval of x corresponds to the
9 estimates of x for CPs in the clusters composing cometary dust and regoliths, which were
10 obtained from modeling the negative branch of polarization permanently observed in comets and
11 atmosphereless bodies (see, e.g., [18-20]). Though we actually calculated the light-scattering
12 models for several cases of the CP sizes, we present here the results only for the CP radius $a =$
13 $0.115 \mu\text{m}$, which corresponds to $x = 1.2$ at $\lambda = 0.60 \mu\text{m}$. Obviously, the change in the CP size
14 does not induce essential changes in the spectral behavior of $F(\pi)$ and only shifts the whole
15 pattern along the spectrum (see below).

16 The shape of particles composing aggregates is assumed to be spherical, since this allows
17 us to distinguish easier the manifestations of properties of individual particles in the scattering
18 characteristics of complex aggregates. This assumption is supported by the results of calculations
19 [20-22] and laboratory measurements [23] of the scattering characteristics of aggregates
20 composed of particles irregular in shape. They show that these characteristics are close to those
21 of aggregates of spherical particles when the CP size parameters are rather small, $x < 2$. This fact
22 is explained by blurring out the peculiarities in the scattering by individual spherical particles of
23 these sizes by near-field effects if they are close to each other in the aggregate.

24 To understand the effect of the structure of clusters on their spectral pattern, we consider
25 relatively densely packed fractal-like clusters with the following fractal parameters: the pre-
26 factor $k_f = 8$ and the fractal dimensions $D_f = 3, 2.5,$ and 2.1 (in the following, structures A, B,
27 and C) and a much fluffier fractal-like cluster with $k_f = 5.8$ and $D_f = 1.9$ (structure D). We define
28 these parameters according to the description given in the paper [24]. The porosity of clusters is
29 determined from the so-called characteristic radius $R_c = (5/3)^{1/2} \times R_g$ [25], where R_g is the
30 gyration radius of a cluster. Then, the porosity is $p = 1 - N \times (a/R_c)^3$, where N is the number of
31 CPs (monomers). For clusters A–D composed of 42 monomers with radii $a = 0.115 \mu\text{m}$ (which
32 corresponds to the volume equivalent sphere with a radius $R = 0.4 \mu\text{m}$), $p = 0.54, 0.67, 0.78,$ and
33 0.93 , respectively. All these structures are shown below in the inset of Fig. 1.

34 Though the structure of the clusters with assumed fractal parameters weakly but depends

1 on realization peculiarities and, consequently, the characteristics of the scattered light are also
 2 realization-dependent [14], we consider here the spectra only for one of the structure realizations.
 3 The reason is that we are interested here only in the qualitative behavior of the spectrum in
 4 dependence on the properties of the clusters, and we do not average the spectrum over
 5 realizations for deriving the quantitative dependence.

6 **3. Spectra of the phase functions of single particles and aggregates: the similarities** 7 **and differences**

8 At the beginning, let us compare the spectral dependences of $F(\pi)$ for randomly oriented
 9 clusters of spherical CPs and individual spherical particles. The phase functions are normalized
 10 in the following way: $F = 4a_{11}/Q_{\text{sca}}/x^2_v$, where a_{11} is the element of the scattering matrix and $x_v =$
 11 x for a single particle or is defined for an aggregate as the size parameter of the equivalent-
 12 volume sphere. The scattering matrix of single homogeneous spherical particles is calculated
 13 with the Lorenz–Mie theory (e.g., [12]). To calculate the scattering matrix of aggregates, we use
 14 the superposition T-matrix method, which is one of the most versatile and efficient direct
 15 computer solvers of the macroscopic Maxwell equations and is widely applied to the
 16 computation of electromagnetic scattering by an arbitrary multi-sphere configuration in random
 17 or fixed orientation [12]. Consequently, we compute the elements of the single-scattering Stokes
 18 matrix for the generated clusters with the corresponding publicly available FORTRAN code
 19 (MSTM) [26].

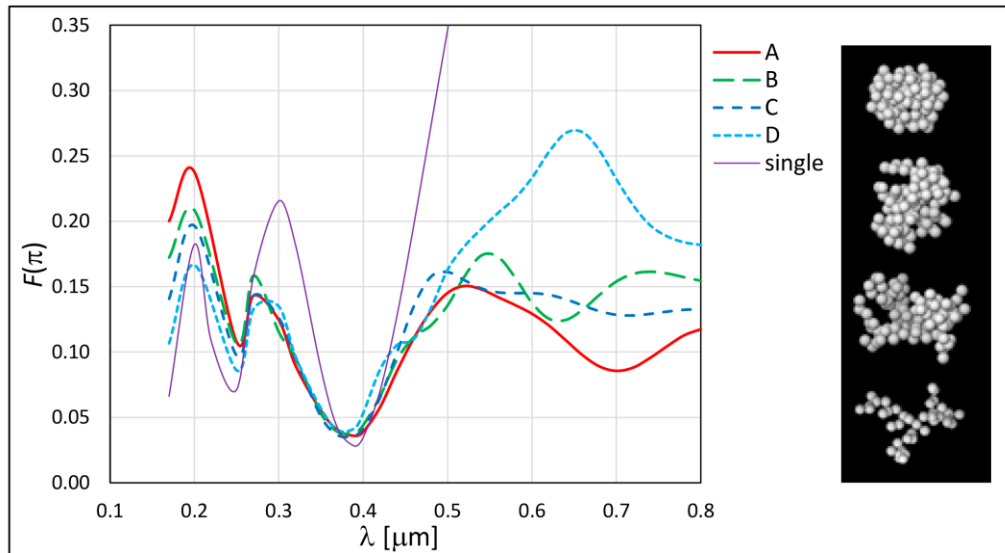


Fig. 1.

20
 21 Fig. 1. The spectral dependences of $F(\pi)$ for single spherical ice particles with a radius of
 22 $0.115 \mu\text{m}$ and for aggregate structures A–D (shown top-down in the inset) composed of such
 23 particles.

1 Figure 1 shows the spectral dependences of $F(\pi)$ for randomly oriented clusters A–D
2 composed of 42 ice CPs with radii $a = 0.115 \mu\text{m}$ and for single spherical ice particles with the
3 same radius as that of CPs. In the short-wavelength range, all structures exhibit similar patterns
4 corresponding to the features in the spectrum of individual monomers. This means that some
5 features in the spectrum of radiation reflected by individual particles survive in the spectrum of
6 their aggregates. At longer wavelengths, where the scattering by single spheres becomes more
7 isotropic and the $F(\pi)$ curve constantly grows, we observe the formation of additional details in
8 the spectra of aggregates. Obviously, they develop due collective effects induced by scattering
9 on CPs in the aggregates.

10 To explain the pattern of the spectra of aggregate particles, we will start from the simplest
11 example of scattering by homogeneous spherical particles. The amplitude matrix \mathbf{S} of the
12 radiation scattered by a homogeneous sphere in the backscattering direction is determined by

$$13 \quad S_1(\pi) = -S_2(\pi) = \frac{1}{2} \sum_n (2n + 1) (-1)^n (a_n - b_n),$$

14 where a_n and b_n are the Mie coefficients [12]. Note that, though these relationship was obtained
15 for the strictly backscattering direction, it is approximately valid for some angular range around
16 this direction. As is seen from the above formula, for some wavelengths and refractive indices
17 and sizes of particles, the intensity of the reflected radiation may be minimal or even vanish. The
18 latter case results from the equal values of the coefficients a_n and b_n . Consequently, the spectral
19 curves for spherical particles of the same size clearly demonstrate the interference behavior with
20 a characteristic series of minima and maxima, which are well seen in Fig. 2. With increasing the
21 real part of the refractive index m_r , the minima and maxima move to the long-wavelength range
22 of the spectrum. We may say that this shift is caused exactly by changing the real part of the
23 refractive index, since the absorption in the particles produces almost no effect on the position of
24 features in the spectrum of the reflected light and only reduces their amplitude.

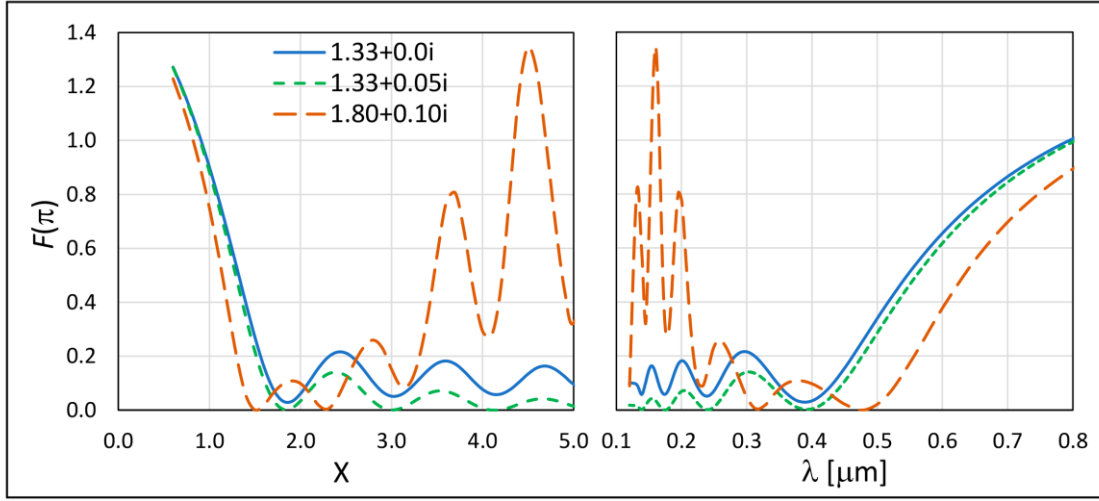


Fig. 2

1
2 Fig. 2. The value of $F(\pi)$ for spherical homogeneous particles of the specified materials in
3 dependence on their size parameter (left) and the wavelength (right); the radius of particles is $a =$
4 $0.115 \mu\text{m}$.

5
6 Though the geometric optics statements may hardly be applied to the considered size
7 parameters, the estimates of the extrema positions on the spectral curves obtained in the frames
8 of such an approach yield reasonable results. Thus, if we assume that maxima and minima on the
9 curves result from the interference of waves, one of which is reflected from the outer surface of
10 the particle while the second one passes through the particle twice and returns backwards, the
11 maximum and minimum positions x_0 on the curve plotted in dependence on the size parameter
12 will be determined as $x_0 = n\pi/4/m_r$. If n takes odd values, this relationship yields the positions of
13 the minima, while the positions of the maxima correspond to even values of n . If $n \geq 3$, this
14 relationship fits the extrema positions for $m_r = 1.33$ quite well, while the agreement becomes
15 worse for $m_r = 1.80$. It is worth noting that this approach may be useful for estimating the sizes
16 or refractive indices of particles from spectral measurements of sparse monodisperse media
17 composed of homogeneous spherical particles (or not strongly differing from spheres) or
18 aggregates of particles of the same sizes.

19 Though we consider here only the clusters of particles with $a = 0.115 \mu\text{m}$, the above
20 formula allows one to determine, at least approximately, the positions of minima and maxima in
21 the spectrum for other values of the CP size and refractive index.

22 Thus, the features observed at short wavelengths in the spectra of aggregates are obviously
23 initiated by the scattering of light on single CPs. To investigate the development of the pattern
24 observed for aggregates at $\lambda > 0.5 \mu\text{m}$, where the scattering on single particles generates no

1 features, simply organized specific systems of particles turned out to be useful.

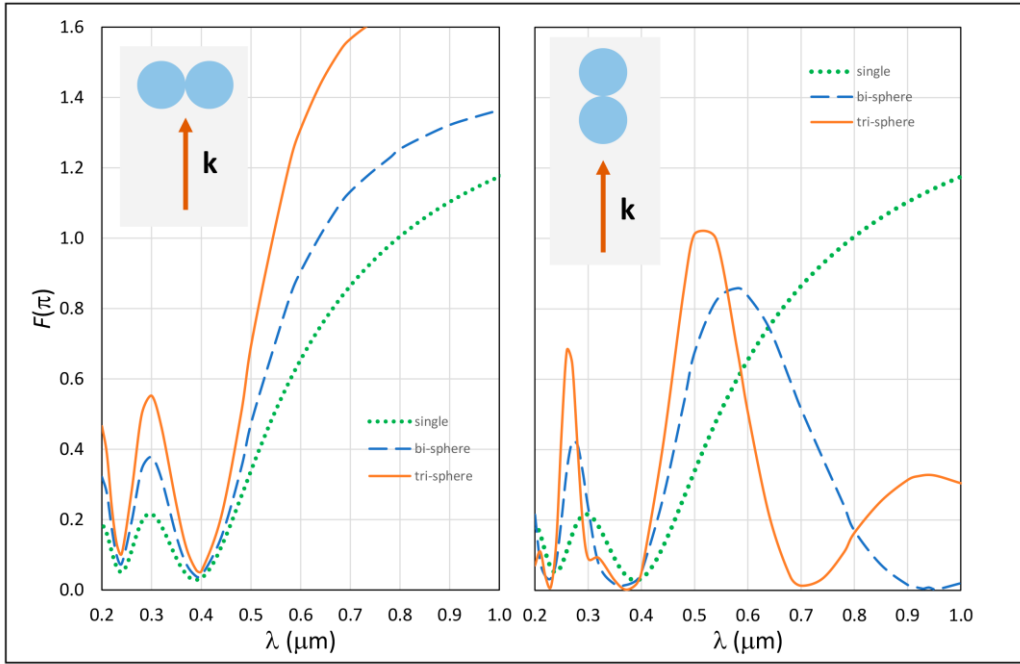


Fig. 3.

2
3 Fig. 3. The spectra of $F(\pi)$ for bi- and tri-spheres in contact, the axes of which are oriented
4 perpendicular to (left panel) and along (right panel) the incident radiation direction \mathbf{k} . The
5 parameters of CPs are $a = 0.115 \mu\text{m}$ and $m = 1.33 + 0.0i$. The spectral curve for single spherical
6 particles of this properties is shown for comparison.

7
8 Figure 3 shows the spectral dependence of $F(\pi)$ for clusters of two and three spherical
9 particles in contact (bi- and tri-spheres), the parameters of constituents of which are $a = 0.115$
10 μm and $m = 1.33 + 0.0i$. Two orientations of the cluster axis relative to the incident radiation
11 direction \mathbf{k} are considered---along and perpendicular to it. The spectra of the clusters in
12 perpendicular orientation to the \mathbf{k} direction are averaged by rotation about \mathbf{k} . As is seen from the
13 figure, when the axes of the bi- and tri-spheres are perpendicular to \mathbf{k} , no additional features in
14 the $F(\pi)$ spectrum appear, and the amplitudes of the initial features, which are connected with the
15 scattering on single spheres, grow due to the increase in the number of scatterers. At the same
16 time, when the axes of the bi- and tri-spheres are oriented along \mathbf{k} , additional interference
17 features appear at $\lambda > 0.4 \mu\text{m}$. It can be shown that the minima near 0.70 and $0.95 \mu\text{m}$ for the tri-
18 and bi-spheres, respectively, are caused by the interference of waves singly scattered by different
19 CPs in the system. If the influence of particles above the frontal one relative to the incident wave
20 were ignored in calculations of the interference, these minima would be formed at 0.69 and 0.92
21 μm , respectively. However, since the wave front immediately behind the frontal particle turns
22 out to be retarded relative to the incident wave front and the near field becomes inhomogeneous

(see, e.g., the structure of the near field in the vicinity of a scatterer in Fig. 1b of a paper [4]), these minima are somewhat shifted to the long-wavelength range and their shape becomes slightly smoothed.

Due to this interference, the additional maximum is also formed; and it becomes more pronounced and moves to short wavelengths with increasing the CP number. At $\lambda < 0.38 \mu\text{m}$, this interference also manifests itself: it shifts the “individual” maximum to shorter wavelengths and makes it narrower with increasing the number of particles. The position of the minimum at $\lambda \approx 0.38 \mu\text{m}$ is determined only by the properties of the CPs and almost independent of the number of CPs.

Let us apply the results of the analysis of spectral features in the spectra of individual spherical particles and bi- and tri-spheres to the explanation of the reflectance spectra of aggregates.

4. Changes in the spectra of aggregates caused by increasing the CP number

Since we may expect that the growth of an aggregate may induce changes in its spectrum, let us consider the influence of the number of CPs on the spectral dependences of $F(\pi)$. Figure 4 shows how the spectra of $F(\pi)$ for clusters B and C change with growing the number of CPs. The analogous dependences for cluster A is in Fig. 5 (left panel). We present examples for the clusters composed of ice monomers with $a = 0.115 \mu\text{m}$ (the quantity R specified in the legends is the radius of the sphere with a volume equal to the sum of volumes of all CPs in the cluster expressed in micrometers).

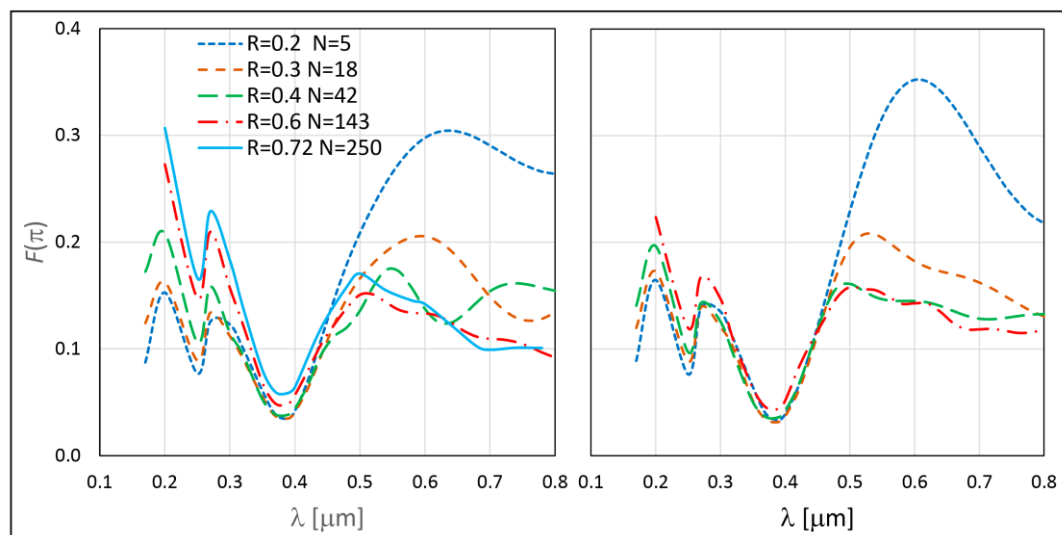


Fig. 4

Fig. 4. Changes in the spectra of $F(\pi)$ for clusters of structures B (left) and C (right) with growing the number of monomers N ; their radius is $a = 0.115 \mu\text{m}$, and the material is H_2O ice.

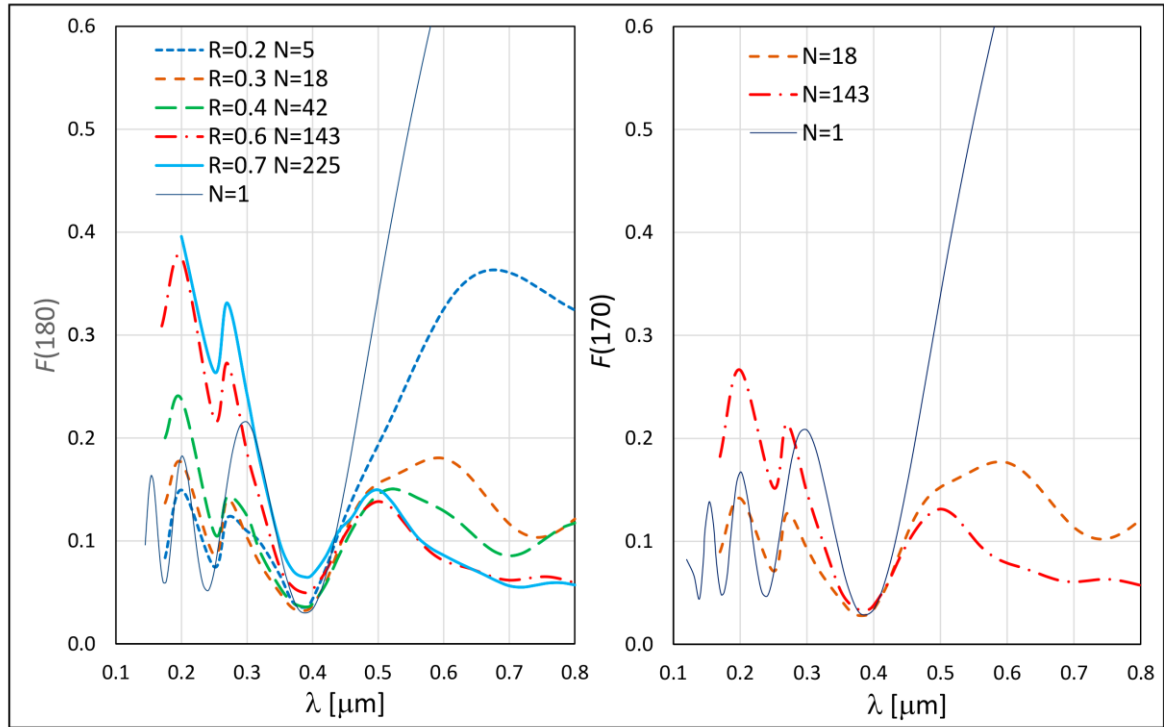


Fig. 5

1
2 Fig. 5. Changes in the spectra of $F(\theta=180^\circ)$ (left) and $F(\theta=170^\circ)$ (right) for clusters of
3 structure A with growing the CP number N ; their radius is $a = 0.115 \mu\text{m}$, and the material is H_2O
4 ice. The spectral curve for a single monomer is shown for comparison.

5
6 As has been already determined, the spectral features in the short-wavelength range are
7 mainly formed by the scattering on individual CPs. At the same time, the intensity of the
8 reflected light grows here with growing the number of CPs. This increase is mainly induced by
9 the weak-localization (opposition) effect. In particular, this follows from the results of our model
10 calculations of the single scattering matrix for aggregates. They show that the linear polarization
11 changes its sign in the back scattering domain as compared to the polarization sign for individual
12 CPs (we do not show here all the results to avoid overloading the figures). For example, at $\lambda =$
13 0.25 and $0.27 \mu\text{m}$, the degree of linear polarization of light scattered by monomers with $a =$
14 $0.115 \mu\text{m}$ near opposition is positive, while it is negative for clusters of this monomers. This
15 inversion of the polarization sign is characteristic of the weak-localization effect (see, e.g.,
16 [13–15, 17, 18] and references therein). Due to the same effect, the intensity of light scattered at
17 $\theta = 170^\circ$ (Fig. 5, right) is lower than that at $\theta = 180^\circ$ (Fig. 5, left).

18 It is worth noting that, in this spectral range, the interference of singly scattered waves also
19 manifests itself: it makes narrower the interference maxima and shifts them to shorter
20 wavelengths (see also Fig. 3).

1 In Figs. 4 and 5, the minimum at 0.38 μm , which is formed by the scattering on individual
2 CPs of the clusters, draws attention. Regardless the structure properties (see also Fig. 1), it barely
3 moves and changes the shape with increasing the number of CPs. Consequently, this minimum
4 may play an important role in estimating the parameters of particles in the clusters from the light
5 scattering characteristics. In particular, from this minimum, one may determine the size of CPs in
6 the clusters (if the refractive index is known) or the refractive index (if the CP size is known).
7 Naturally, this inference is correct only to the media, where composing aggregates are in the far
8 zones of each other.

9 At longer wavelengths, at $\lambda > 0.50 \mu\text{m}$, the second noteworthy feature develops with
10 increasing the number of CPs: it is the maximum analogous to that observed for the bi- and tri-
11 spheres in Fig. 3. In this spectral range, the shape of the curve strongly depends on the CP
12 number; and, for a rather large number of CPs, the curve becomes insensitive to its further
13 increase. For aggregates B and C the maxima at $\lambda \approx 0.50 \mu\text{m}$ are less expressed than that for
14 structure A, and the spectral curve at wavelengths $\lambda > 0.50 \mu\text{m}$ becomes weakly declining or
15 almost flat with growing N , which is explained by averaging the spectrum over several rather
16 densely packed fragments of the aggregates.

17 We consider the maximum appeared at $\lambda \approx 0.50 \mu\text{m}$ in the spectra of the examined
18 aggregates as manifestation of collective effects caused by the interference of waves singly
19 scattered by CPs in the aggregates (see also Fig. 3). There are more groups of particles as bi- and
20 tri-spheres in more densely packed clusters than in fluffier ones with the same number of CPs.
21 Consequently, cluster A exhibits the best developed “collective” maximum near 0.50 μm . This
22 maximum becomes almost resistant to the further growth of N in cluster A already at $N = 42$,
23 while the fluffy cluster D with $N = 42$ exhibits the collective maximum still at long wavelengths
24 (see Fig. 1), where the maximum for the much smaller cluster A is observed.

25 The influence of different sizes of CPs in clusters was examined by an example of
26 structures constructed in the following way. Since such clusters cannot be built with fractal
27 relationships, we filled a specified volume with spherical particles of different sizes. Their radii
28 were randomly varied around the assumed mean value with a difference ranging within $d =$
29 $\pm 10\%$. We used the volume of a slightly “distorted” sphere, since the considered fractal-like
30 clusters are more or less equidimensional, but we tried to avoid the wavy spectral features
31 induced by scattering on a large spherical particle. We chose the distorting function that affects
32 the radial position r_i of the i th CP, which is put into the volume in dependence on the angles of
33 the spherical coordinate system θ_i and φ_i . Namely, $r_i = \text{rand}(R - a_i) * (1 + f(\theta_i, \varphi_i) \times \cos^2 \theta_i \times$

1 $\cos^2(\varphi_i)$, where $f(\theta_i, \varphi_i)$ was chosen in a different way in different realizations.

2 The number of CPs and the packing density were specified according to the values for a
3 rather densely packed cluster of structure A. The size of the “quasi-sphere”, being filled up, was
4 varied until the required packing density of the polydisperse cluster was obtained. Then, the
5 same volume was filled up with spherical particles with sizes differing within a range of $d =$
6 $\pm 20\%$; the obtained packing density of CPs in this cluster was smaller than in the previous case.
7 To reach the same packing density, we decreased the filled volume. Thus, on the basis of the
8 packing densities of two fractal-like clusters of type A composed of 42 and 143 monomers, we
9 constructed one polydisperse cluster with $d = \pm 10\%$ and two polydisperse clusters, differing in
10 size and packing density, with $d = \pm 20\%$ for each of them.

11 As one may expect, variations in the sizes of CPs in the above described aggregates
12 substantially smooth the short-wavelength features that are caused by the interference of light
13 scattered by individual CPs. The minimum near $0.38 \mu\text{m}$ may simultaneously be shifted to the
14 short-wavelength range, and the wider the range of CP sizes, the shallower this minimum. At the
15 same time, the collective maximum at longer wavelengths survives (see Fig. 6).

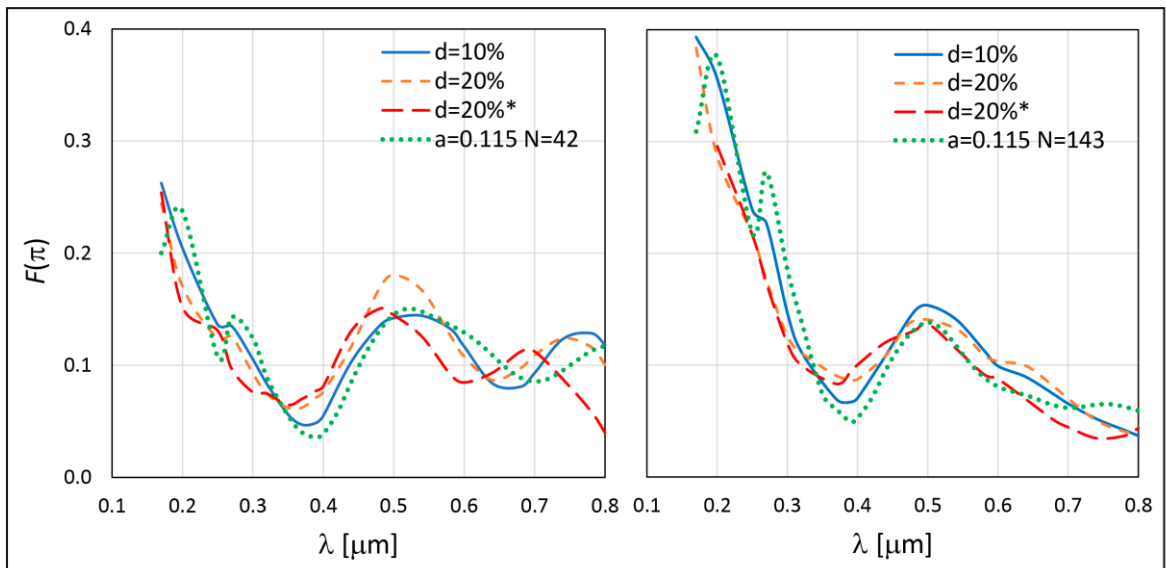


Fig. 6

16

17 Fig. 6. The spectral dependence of $F(\pi)$ for clusters composed of polydisperse spherical ice
18 particles; the number of CPs is $N = 42$ (left) and 143 (right). The deviations in the CP sizes from
19 the mean value ($a = 0.115 \mu\text{m}$) are within $d = \pm 10$ and 20% (the star marks the smaller cluster
20 (see text)). The spectral curves for the clusters of structure A, containing the same number of
21 identical CPs, are shown for comparison.

22

23

1 **4. Concluding remarks**

2 In this paper we examined the manifestations of collective effects in the visible spectrum
3 of the intensity of light scattered by aggregate structures of submicron spherical particles. For
4 this, we compared the model spectra of light scattered by different ensembles of particles and
5 their individual constituents.

6 The results of the superposition T-matrix calculations showed that the spectra of randomly
7 oriented fractal-like aggregates contain the interference extrema characteristic of individual
8 constituents, and their positions in the spectra expectedly depends on the refractive index and the
9 sizes of CPs. At longer wavelengths, where the intensity of light scattered by individual particles
10 constantly grows, an additional maximum appears in the spectra of aggregates. We consider this
11 maximum as manifestation of collective effects in aggregate structures caused by the
12 interference of waves singly scattered by different CPs in the ensembles. In the spectra of
13 randomly oriented aggregates, the position of this maximum, starting from some number of CPs,
14 becomes almost resistant to the further aggregate growth and dependent only on the refractive
15 index and sizes of CPs. The collective maximum survives even in the spectra of clusters with
16 CPs of slightly varied sizes, while the interference features induced by individual constituents
17 naturally become smoother.

18 It is worth noting that the most expressed minimum caused by the scattering at individual
19 CPs in clusters, which is closest to the collective maximum, is not much sensitive to variations in
20 the sizes of CPs within the clusters and strongly resistant to changes in the aggregate structure
21 and CP number. Consequently, even in the case of somewhat differing CP sizes, it may serve for
22 estimating the parameters of particles in the aggregates from the spectra measured for the media,
23 where aggregates are in the far zones of each other.

24 **Acknowledgments**

25 The authors are grateful to D. Mackowski and M. Mishchenko for making available the
26 superposition T-matrix (MSTM) computational code
27 (<https://www.eng.auburn.edu/~dmckwski/scatcodes/>,
28 https://www.giss.nasa.gov/staff/mmishchenko/t_matrix.html) and to the reviewers for
29 constructive remarks.
30

31 **Funding**

32 The work by V.P. Tishkovets was supported by the Marie Skłodowska-Curie Research
33 Innovation and Staff Exchange (RISE) (the GRASP-ACE grant no. 778349).
34

References

- [1] Bhowmik A, Pilon L. Can spherical eukaryotic microalgae cells be treated as optically homogeneous. *J Opt Soc Am A* 2016;33:1495–503. doi: 10.1364/JOSAA.33.001495.
- [2] Glotch TD, Bandfield JL, Wolff MJ, Arnold JA, Che C. (2016), Constraints on the composition and particle size of chloride salt-bearing deposits on Mars. *J Geophys Res Planets* 2016;121:454–71. doi:10.1002/2015JE004921.
- [3] Kimura H. High radiation pressure on interstellar dust computed by light-scattering simulation on fluffy agglomerates of magnesium–silicate grains with metallic-iron inclusions. *Astrophys J Lett* 2017;839:L23. <https://doi.org/10.3847/2041-8213/aa6c2d>.
- [4] Tang GH, Bi C, Zhao Y, Tao WQ. Thermal transport in nano-porous insulation of aerogel: factors, models and outlook. *Energy* 2015;90:701–21. <https://doi.org/10.1016/j.energy.2015.07.109>.
- [5] Rasskazov IL, Spegazzini N, Carney PS, Bhargava R. Dielectric sphere clusters as a model to understand infrared spectroscopic imaging data recorded from complex samples. *Anal Chem* 2017; 89:10813–18. DOI: 10.1021/acs.analchem.7b02168.
- [6] Tamanai A, Vogt J, Huck Ch, Mick U, Zimmermann S, Tazaki R, Mutschke H, Pucci A. Experimental verification of agglomeration effects in infrared spectra on micron-sized particles. *Astron Astrophys* 2018;619:A110. <https://doi.org/10.1051/0004-6361/201833119>.
- [7] Ysard N, Jones A P, Demyk K., Boutéraon T, Koehler M. The optical properties of dust: the effects of composition, size, and structure. *Astron Astrophys* 2018;617:A124. <https://doi.org/10.1051/0004-6361/201833386>.
- [8] Ohno K, Okuzumi S, Tazaki R. Clouds of fluffy aggregates: How they form in exoplanetary atmospheres and influence transmission spectra. *ApJ* 2019; accepted for publication, arXiv:1908.02201 [astro-ph.EP]. DOI: 10.3847/1538-4357/ab44bd.
- [9] Mishevich AA, Loiko VA. Two-dimensional planar photonic crystals: calculation of coherent transmittance and reflectance at normal illumination under the quasicrystalline approximation. *J Quant Spectrosc Radiat Transfer* 2011;112:1082–9. <https://doi.org/10.1016/j.jqsrt.2010.11.019>.
- [10] Loiko VA, Mishevich AA. Multiple scattering of light in ordered particulate media. In: Kokhanovsky AA, editor. *Springer Series in Light Scattering*, Springer, Cham; 2018, p. 101–230. https://doi.org/10.1007/978-3-319-70796-9_2.
- [11] Loiko NA, Mishevich AA, Loiko VA. Incoherent component of light scattered by a monolayer of spherical particles: analysis of angular distribution and absorption of light. *J Opt Soc Am A* 2018; 35:1:108–18. <https://doi.org/10.1364/JOSAA.35.000108>.
- [12] Mishchenko MI, Travis LD, Lacis AA. *Scattering, absorption, and emission of light by small particles*. Cambridge: Cambridge University Press; 2002.
- [13] Mishchenko MI, Liu L, Mackowski DW, Cairns B, Videen G. Multiple scattering by random particulate media: exact 3D results. *Opt Express* 2007;15:2822–36. <https://doi.org/10.1364/OE.15.002822>.
- [14] Tishkovets VP, Petrova EV, Jockers K. Optical properties of aggregate particles comparable in size to the wavelength. *J Quant Spectrosc Radiat Transfer* 2004;86(3):241–65. <https://doi.org/10.1016/j.jqsrt.2003.08.003>.
- [15] Petrova EV, Tishkovets VP, Jockers K, Interaction of particles in the near field and

- 1 opposition effects in regolith-like surfaces. *Solar Syst Res* 2009;43:100–15.
2 <https://doi.org/10.1134/S0038094609020026>.
- 3 [16] Kolokolova L, Petrova E, Kimura H. Effects of interaction of electromagnetic waves in
4 complex particles. In: Zhurbenko V, editor. *Electromagnetic Waves*, IntechOpen, DOI:
5 10.5772/16456. Available from: [https://www.intechopen.com/books/electromagnetic-](https://www.intechopen.com/books/electromagnetic-waves/effects-of-interaction-of-electromagnetic-waves-in-complex-particles)
6 [waves/effects-of-interaction-of-electromagnetic-waves-in-complex-particles](https://www.intechopen.com/books/electromagnetic-waves/effects-of-interaction-of-electromagnetic-waves-in-complex-particles).
- 7 [17] Petrova EV, Tishkovets VP. Light scattering by morphologically complex objects and
8 opposition effects (a review). *Solar Syst Res* 2011;45:304–22.
9 <https://doi.org/10.1134/S0038094611030038>.
- 10 [18] Petrova EV, Tishkovets VP, Jockers K. Polarization of light scattered by Solar System
11 bodies and the aggregate model of dust particles. *Solar Syst Res* 2004;38:309–24.
12 <https://doi.org/10.1023/B:SOLS.0000037466.32514.fe>.
- 13 [19] Kimura H, Kolokolova L, Mann I. Light scattering by cometary dust numerically simulated
14 with aggregate particles consisting of identical spheres. *Astron Astrophys* 2006;449:1243–
15 54. DOI: 10.1051/0004-6361:20041783.
- 16 [20] Lumme K, Penttilä A. Model of light scattering by dust particles in the solar system:
17 Applications to cometary comae and planetary regoliths. *J Quant Spectrosc Radiat Transfer*
18 2011;112:1658–70. DOI: 10.1016/j.jqsrt.2011.01.016.
- 19 [21] Xing Z, Hanner M. Light scattering by aggregate particles. *Astron Astrophys* 1997;
20 324:805–20.
- 21 [22] Zubko E, Shkuratov Yu, Videen G. Effect of morphology on light scattering by
22 agglomerates. *J Quant Spectrosc Radiat Transfer* 2015;150:42–54.
23 <http://dx.doi.org/10.1016/j.jqsrt.2014.06.023>.
- 24 [23] Gustafson BÅS, Kolokolova L. A systematic study of light scattering by aggregate particles
25 using the microwave analog technique: Angular and wavelength dependence of intensity
26 and polarization. *J Geophys Res* 1999;104:D24:31711–20. DOI: 10.1029/1999JD900327
- 27 [24] Mackowski DW. Electrostatics analysis of sphere clusters in the Rayleigh limit: application
28 to soot particles. *Appl Opt* 1995;34:3535–45. <https://doi.org/10.1364/AO.34.003535>.
- 29 [25] Kosaza T, Blum J, Okamoto H, Mukai T. Optical properties of dust aggregates. 1.
30 Wavelength dependence. *Astron Astrophys* 1992;263:423–32.
- 31 [26] Mackowski DW, Mishchenko MI. A multiple sphere T-matrix Fortran code for use on
32 parallel computer clusters. *J Quant Spectrosc Radiat Transfer* 2011;112:2182–92.
33 <http://dx.doi.org/10.1016/j.jqsrt>.

34
35 **Figure captions**

36 Fig. 1. The spectral dependences of $F(\pi)$ for single spherical ice particles with a radius of
37 $0.115 \mu\text{m}$ and for aggregate structures A–D (shown top-down in the inset) composed of such
38 particles.

39 Fig. 2. The value of $F(\pi)$ for spherical homogeneous particles of the specified materials in
40 dependence on their size parameter (left) and the wavelength (right); the radius of particles is $a =$
41 $0.115 \mu\text{m}$.

42 Fig. 3. The spectra of $F(\pi)$ for bi- and tri-spheres in contact, the axes of which are oriented

1 perpendicular to (left panel) and along (right panel) the incident radiation direction \mathbf{k} . The
2 parameters of CPs are $a = 0.115 \mu\text{m}$ and $m = 1.33 + 0.0i$. The spectral curve for single spherical
3 particles of this properties is shown for comparison.

4 Fig. 4. Changes in the spectra of $F(\pi)$ for clusters of structures B (left) and C (right) with
5 growing the number of monomers N ; their radius is $a = 0.115 \mu\text{m}$, and the material is H_2O ice.

6 Fig. 5. Changes in the spectra of $F(\theta=180^\circ)$ (left) and $F(\theta=170^\circ)$ (right) for clusters of
7 structure A with growing the CP number N ; their radius is $a = 0.115 \mu\text{m}$, and the material is H_2O
8 ice. The spectral curve for a single monomer is shown for comparison.

9 Fig. 6. The spectral dependence of $F(\pi)$ for clusters composed of polydisperse spherical ice
10 particles; the number of CPs is $N = 42$ (left) and 143 (right). The deviations in the CP sizes from
11 the mean value ($a = 0.115 \mu\text{m}$) are within $d = \pm 10$ and 20% (the star marks the smaller cluster
12 (see text)). The spectral curves for the clusters of structure A, containing the same number of
13 identical CPs, are shown for comparison.

14